

## Chapter 3

# Modelling spatial memory

**Abstract** Among the different capabilities of animals, the formation of spatial memories is crucial for their life. Living beings able to move, constantly need to orient themselves in the environment to reach a target that might be not always visible. This chapter investigates the process of spatial memory formation as an essential ingredient for orientation in open and unstructured environments. Neural centres devoted to spatial memory and path integration were deeply investigated in both rats and different insect species like ants, bees and fruit flies. In this chapter a neural-inspired model for the formation of a spatial working memory is discussed considering some key elements of the insect neural centres involved, in particular the ellipsoid body of the central complex.

### 3.1 Introduction

Visual place learning and path integration are relevant capabilities for autonomous robotic systems. Probing into bio-inspired solutions within the animal world, insects like ants and fruit flies can walk in complex environments using different orientation mechanisms: for tracking temporarily obscured targets and for reaching places of interest like a food source, a safe place or the nest. For species that construct nests, the homing mechanisms are fundamental. In the case of desert ants, the route to the nest can be found also after long foraging travels in unstructured environments [18]. In this case, mechanisms of path integration are important to avoid accuracy problems [5]. Landmark navigation can be used to compensate the cumulative errors typical of odometric-based strategies [7].

Neural structures based on mutually coupled populations of excitatory and inhibitory neurons were used to model the navigation behaviour of desert ant [10]. The formation of activity bumps within the neuron populations is used to embed the system orientation in the neural structure. Different mathematical formulations were also considered based on the sinusoidal arrays that condensate the representation of the information using vectors [19]. Besides path integration, interesting approaches

for landmark navigation were developed using recurrent neural networks [8] and vision-based strategies that involve population of circular array cells [9].

Together with insects, rats were a useful source of inspiration. In these animals the head direction is codified in cells of the limbic system [17, 15]. While moving in the environment, the animal internally encodes its orientation using a persistent hill of neural activity in a ring-shaped population of excitatory neurons. The position of the activity peak is shifted while turning, using the angular head velocity that is provided as input to other two rings of inhibitory neurons [17].

As previously introduced, insects are able to use spatial information to memorize visual features (spatial distribution, color, etc.) so that they can return to interesting places and can avoid dangerous objects. Furthermore, also insects are able to solve a problem similar to the famous Morris water maze problem [14], i.e. an experimental setup where the animal is forced to reach a safe, invisible place in an tank, relying only on external (extra-maze) cues. In insects, the neural circuits responsible for these behaviours need to be further analysed.

The idea to consider *Drosophila melanogaster* as a model organism has been introduced since chapter 1: it is followed here and in the following chapters. This insect species is particularly interesting for the possibility to apply genetic manipulation tools, to identify the neural processes at the basis of a specific behaviours to be further implemented and demonstrated in bio-inspired robots. Concerning the formation of spatial working memories, even if flies do not create a nest, targeting behaviours are continuously used. Therefore, retaining and recalling a targets position is needed especially when this disappears for a short time.

One experiment used to demonstrate the fly's capabilities in spatial orientation is performed using the detour paradigm where the presentation of a distracter allows to evaluate the robustness of the developed spatial memory also in presence of disturbances [13, 12]. The available genetic manipulation tools identified the important role of the central complex and in particular of the ellipsoid body (EB) in the spatial memory formation process.

In this chapter, on the basis of the neural model proposed in [17] and directly related to orientation in mammals, an adaptation to the insect EB structure has been considered including a further processing level needed for the exploitation of the spatial information contained in the spiking neural structure [2]. Further research led to the discovery of such behaviours as landmark orientation and path integration in specific neural structures within the fruit fly ellipsoid body [16].

## 3.2 Ellipsoid body model

To model the creation of a spatial working memory in the ellipsoid body, three populations of interconnected neurons have been considered.

We took inspiration from other existing models where a concentration of spiking activity in a part of the network is used to store the heading position of the system acquired through proprioceptive sensors [10, 1].

The model contains one population of excitatory cells ( $N_E = 20$ ) and two populations of inhibitory cells ( $N_{I1} = 20$  and  $N_{I2} = 20$  neurons). The neuron model considered for the simulation was the Leaky Integrate and Fire whose characteristics were underlined in chapter 2. The number of neurons considered for the modelling purposes is related to the known neurobiological information on the central complex in *Drosophila* [21] as also briefly discussed in chapter 1. Neurons in each population are labelled by their heading directions and distributed on a ring that follows the EB circular shape.

The connection weights among neurons depend on their mutual angular positions in the chain. A scheme of the network is reported in Fig. 3.1 where the three neural populations together with the connection topology and the external inputs are illustrated.

Each inhibitory neuron has all-to-all connections between other neurons of the same type, with synaptic weights that follow the distribution reported in Fig. 3.2. The excitatory neurons have all-to-all connections with the inhibitory populations with a weight profile reported in Fig. 3.2, whereas each neuron of the inhibitory population is connected with only one neuron of the excitatory population: the neuron that corresponds to the angle  $\theta + \theta_0$  in population  $I_1$ , inhibits the excitatory neuron that corresponds to the angle  $\theta$ ; this receives also a current contribution from the neuron labeled with  $\theta - \theta_0$  in population  $I_2$ . In the original model the connection scheme included all-to-all connections also for the interaction between these layers [17]; the simplification presents minimum drawbacks in terms of level of noise in the network as will be presented in the simulations.

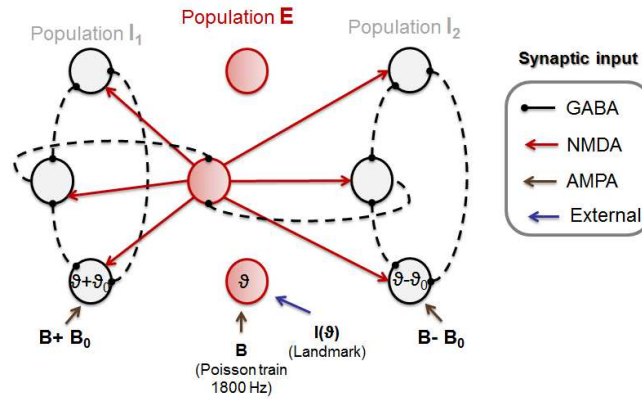


**Fig. 3.1** Simple scheme of the EB model: one population of excitatory (E) and two populations of inhibitory ( $I_1$  and  $I_2$ ) neurons are indicated. Excitatory connections are mediated by AMPA and NMDA receptors whereas GABA is considered for inhibitory connections. In the model a Poisson spike train at 1800 Hz is provided as input to all the network neurons. The presence of a landmark is modelled with a constant input to a given angular position. All-to-all connections between the inhibitory neurons are considered in the model.

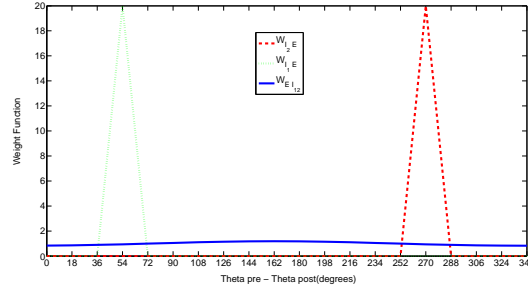


**Fig. 3.2** Weight distribution for the synaptic connections involving the neuron population  $E$ ,  $I_1$  and  $I_2$ . This figure was reprinted from [2], Copyright (2013), with permission from IEEE.

Details on the synaptic connections models via NMDA receptors and parameters are reported in [17] in relation to mammals. However, the presence of several receptors, including NMDA [11] was identified in the fly central complex. Moreover the role of NMDA receptors for long-term memory consolidation in the ellipsoid body was assessed[20].

The network receives information on the angular velocity that is integrated through neural processing to provide step-by-step the system orientation.

The angular velocity signal is provided to the network using an uncorrelated Poisson spike train  $B$  with basic frequency  $f = 1800Hz$  (see fig3.1). Experiments with other spiking distributions (e.g. regular train) were also carried out obtaining similar results. During a rotation performed by the system, the corresponding angular speed is acquired by the network, giving rise to an unbalance between the input on the two inhibitory populations.

The frequency bias ( $B_0$ ) used in this case has been characterized through simulations as shown in Fig. 3.6. Finally an external input current (i.e.  $I(\theta)$ ) can be assigned to a neuron in the excitatory population to indicate the presence of a landmark in a specific angular position. The behaviour of the network consists of a shift of the hill of activity to reach the landmark position.

The first experiments performed with the proposed model were designed in absence of sensory and/or self-motion signals: in this case the insect heading is assumed as fixed. In our model, this is implemented by setting to zero ( $B_0 = 0Hz$ ) the head velocity bias of the external afferent inputs provided to the two inhibitory populations. The network, without external stimuli, quickly reaches a steady state condition with a bell-shaped activity profile. The symmetries of the network do not allow to predict where the peak of the activity hill can arise (i.e. depending on the initial conditions, level of noise, etc.). The absence of synaptic connections in the excitatory population indicates that the hill of activity is generated and maintained by the combination of the external excitatory input and the internal inhibitory input coming from the populations  $I_1$  and  $I_2$ . When the frequency bias  $B_0$  is positive

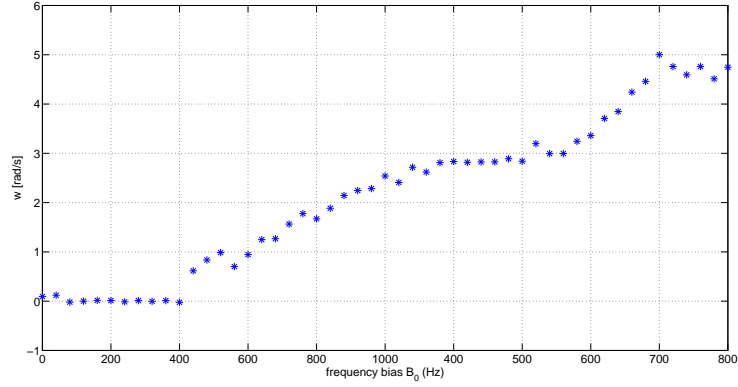


**Fig. 3.3** Relation between the frequency bias ( $B_0$ ) in the Poisson-spike-train and the correspondent angular velocity of the hill of activity in the ring neurons.

(negative) a clockwise (anti-clockwise) rotation of the hill of spiking activity is determined.

The presence of visual landmarks is modelled with an input current in the excitatory population in correspondence to the landmark position. The landmark can be also used as a calibration mechanism to shift the hill to a specific position used as reference point. During movements the accumulated error can be compensated using visual landmarks placed in known positions.

The developed architecture is able to store the animal's heading direction through a bell-shaped activity profile in the excitatory population. To solve more complex tasks like the detour paradigm [13], a spatial integration of the distance travelled by the agent is required. For the sake of simplicity we consider two basic motion behaviours: forward movement and turning on the spot.

An additional ring of neurons (i.e. population P) has been added to the excitatory population to work as a path integrator. These neurons were modelled with a simple linear transfer function. A scheme of the adapted network is reported in Fig. 3.4 where four distinct populations of neurons are considered. The synaptic connections used to connect population E and population P neurons, are supposed to be characterized by a facilitating dynamics as introduced in chapter 2:

$$\dot{u}_n = U - u/F + k\delta_n(t - t_s)\delta(B_0) \quad (3.1)$$

where  $n = 1..N$ ,  $U=0$ ,  $F$  is a fading factor and  $k$  is a gain related to the system speed,  $\delta_n(t - t_s)$  represents the spikes emitted at time  $t_s$  by neurons of population E.

A particularity of the proposed model is the presence of a gating function ( $\delta(B_0)$ ) that allows the contribution of a spike at time  $t_s$  only if the system is in forward motion (i.e.  $B_0 = 0Hz$ ). When the system is turning, the population P is not activated because the action is performed without spatial translation. The parameter  $F$  repre-

sents the rate of discharge of the synaptic state variable and has been fixed to a value that allows to retain the information in a time window of about 5s as also shown in the biological case [13].

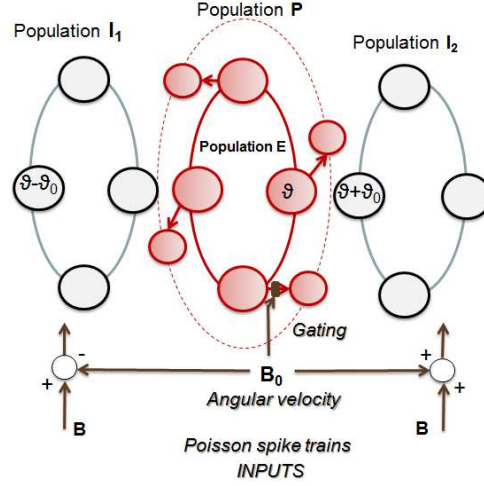


**Fig. 3.4** Extension of the network with the introduction of a fourth ring needed to perform the detour experiments. Population P is used to integrate the forward motion using a gating function that mediates the activity avoiding to consider turning-on-the-spot manoeuvres.

### 3.3 Model simulations

The capabilities of the proposed neural structure were evaluated through a series of simulations. The first experiments consist of the positioning the hill of activity on a fixed reference angle to initialize the network dynamics. The symmetry of the structure determines a variable spatial distribution of the initial hill that depends on the initial conditions. To force the formation in a given position, the landmark is applied on a neuron coding the spatial orientation. In Fig. 3.5 the average firing rate within populations  $E$  and  $I_1$  is shown. The behaviour of population  $I_2$  is similar to  $I_1$  but slightly shifted in order to create two boundaries on the two sides of the population  $E$  blocking the hill of activity in a narrow area. A landmark is applied for a time of 0.5s to the neurons next to  $180^\circ$  through an input current formulated as a Gaussian function:

$$I = Ae^{-\frac{(\vartheta - \vartheta_0)^2}{2\sigma^2}} \quad (3.2)$$

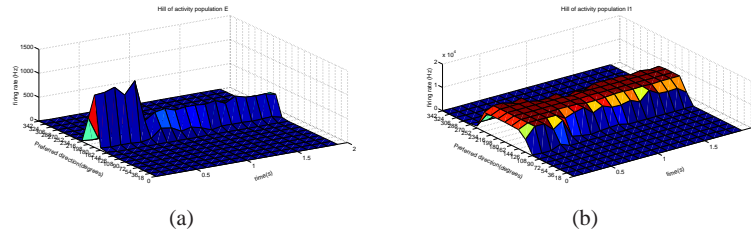


**Fig. 3.5** Time evolution of the firing rate in the population  $E$  and  $I_1$ . The behaviour of  $I_2$  is similar to  $I_1$  with a shift on the other side with respect to population  $E$ . An external input used as landmark, is applied for  $0.5s$  allowing the hill formation in a specific area of the ring. This figure was reprinted from [2], Copyright (2013), with permission from IEEE.

where  $A = 9.4nA$ ,  $\sigma = 24^\circ$  and  $\vartheta_0 = 180^\circ$ .

The effect of a bias current  $B_0$  applied for  $1s$  in order to unbalance the network activity is reported in Fig. 3.6 where the shift of the hill of activity of population P is reported.

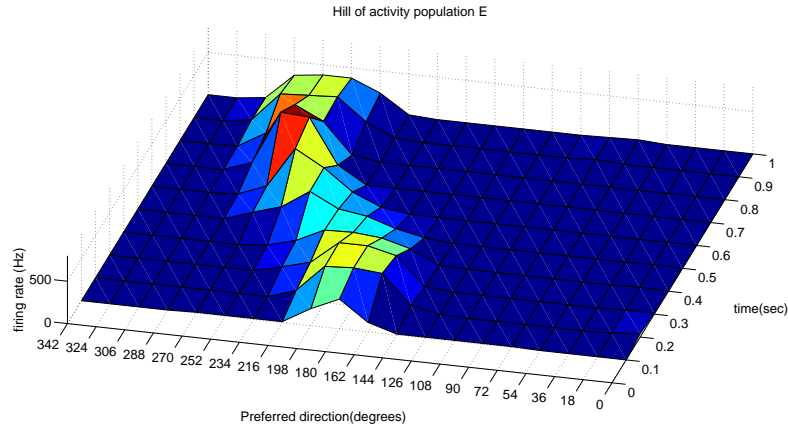


**Fig. 3.6** Effect of an unbalance in the external input frequency distribution. A movement of the spiking activity of the excitatory neurons arises.

An important difference with respect to other works [17] consists of the reduction of synaptic connections between layers creating a more local than global network. Moreover, the reduced number of neurons in the rings can produce residual activity in some neurons far from the hill that in any case does not compromise the stability of the system behaviour.

Population P integrates the activity of population E depending on the robot speed that is used as a gain ( $k$  in eq. 3.1). A calibration procedure is used to find the gain

value that converts the neural activity into a distance travelled expressed in a generic measurement unit.

To further evaluate the system performance, the network was stimulated simulating a forward movement for 1s followed by a rotation of  $130^\circ$  and a second forward action for another 1s; a constant speed of  $1m/s$  was considered. The angular velocity was provided to the network through a  $B_0 = 920Hz$  for 0.5s. A landmark was also provided to guide the initial formation of the hill in a position around  $0^\circ$ . The network, working as a short-term spatial memory, provides as output the estimated position and orientation of the agent.

During the rotation the population P is disconnected from population E using the gating parameter  $k = 0$  in eq. 3.1 and the rotation is considered on the spot (see eq. 3.1). The network integrates in time the speed movement of the agent making an estimation of its spatial position. The heading angle stored by the system during the 3s simulation is reported in Fig. 3.7. The normalized activity of population P that integrates in time the state of population E, is shown in Fig. 3.8. To obtain, step by step, the internally estimated current position of the agent, a vectorial summation is performed considering neurons in population P as polar representation of spatial vectors.

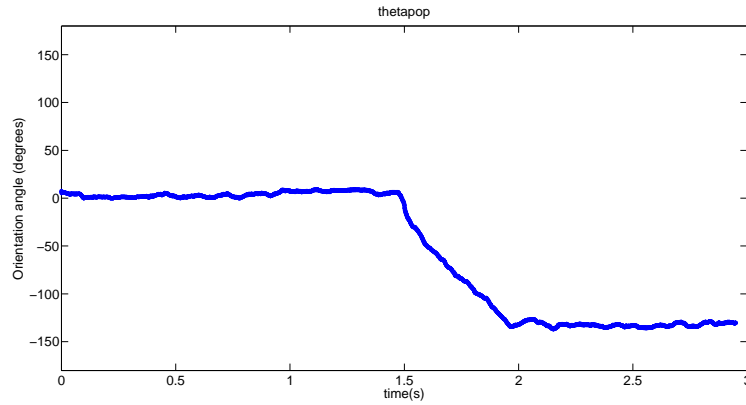


**Fig. 3.7** Time evolution of the heading angle of an agent during a 3s simulation, while performing a forward movement, a turning on the spot of  $130^\circ$  and a second forward movement. This figure was reprinted from [2], Copyright (2013), with permission from IEEE.

A comparison between the real trajectory and the internally memorized one for a complex trajectory containing several straight lines and rotations, is reported in Fig. 3.9. The cumulated error is a consequence of the realistic processing structure and in particular it is due to the relatively low number of neurons distributed in the rings that determine the spatial resolution (i.e. about  $18^\circ$  each neuron).

Therefore, the bio-inspired neural structure can be improved for robotic applications by increasing the spatial resolution to obtain better performance. The be-

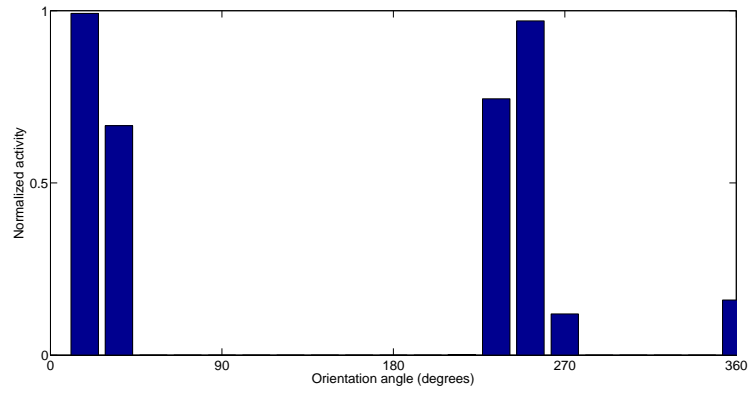


**Fig. 3.8** Normalized activity of population P distributed in the different angular positions. The estimated final position of the agent is evaluated through a simple vectorial sum of the neural activities expressed in a polar coordinate system. This figure was reprinted from [2], Copyright (2013), with permission from IEEE.

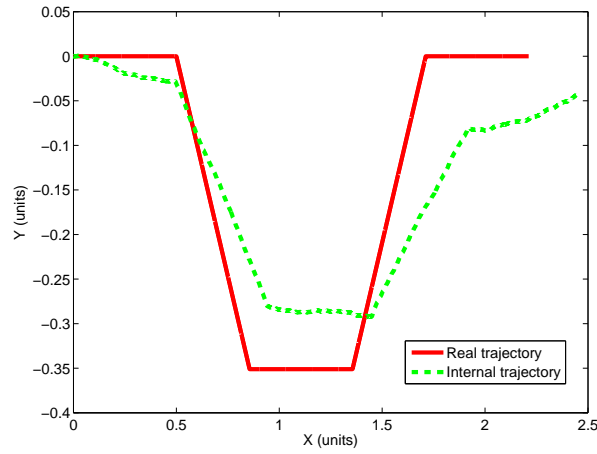


**Fig. 3.9** Comparison between the real trajectory followed by the agent and the internal estimated position stored in the EB.

haviour of the system can be appreciated also in standard tests used in robotics like navigation on a square path [6]. In this simulation each rotation of  $90^\circ$  corresponds to a  $B_o = 800Hz$  applied for  $0.5s$ , and each segment to a forward movement at  $1 \text{ unit/s}$  for  $0.5s$ . In Fig. 3.10 the real trajectory is compared with the step-by-step estimated position provided by the network.

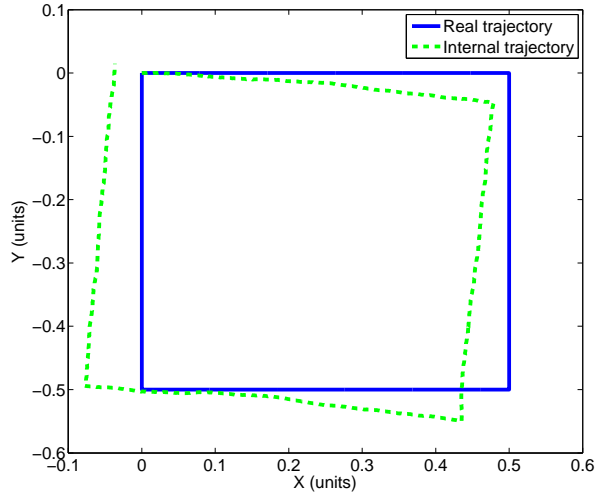


**Fig. 3.10** Comparison between the real trajectory followed by the agent while performing a squared path and the estimated position stored in the EB. This figure was reprinted from [2], Copyright (2013), with permission from IEEE.

To compare the network behaviour with the insect experiments, the detour paradigm was reproduced.

The visually guided navigation in flies is mainly dependent on the central complex. When a target disappears from the scene and a new attractive object appears (i.e. a distractor), the insect stores in the EB neural structure the estimated spatial position of the obscured target that was followed in the previous time window. This estimation can be obtained using corollary discharge (efference copy) of self-motion. Distance is coded using, as measurement unit, the number of steps estimated to reach the object [4, 3]. This spatial vector is coded in the neural population P. The trajectory followed while the insect is attracted by the distractor is integrated in the network to allow the recovery of the original target position within a limited time due to the fading memory.

Three different steps can be distinguished for the simulation:

1. when the target disappears, the EB stores the target estimated position in polar coordinates charging the corresponding neuron of population P with a current proportional to the distance (coded in number of steps);

2. then the hill of activity of population E is forced to arise in a position rotated by  $180^\circ$ . Subsequently the path followed during the presence of a distractor placed at  $90^\circ$  is memorized;
3. when the distractor disappears, the information accumulated in population P is used to estimate the spatial position of the first target.

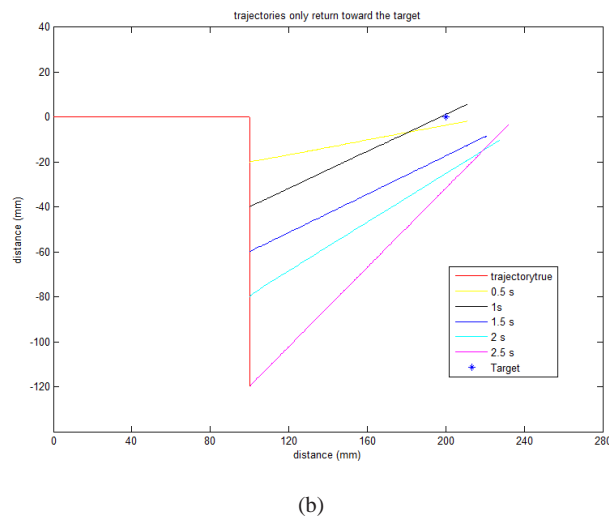
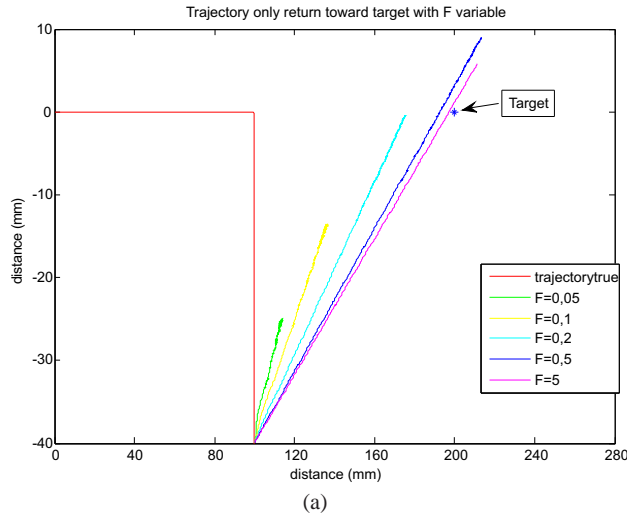


**Fig. 3.11** Detour experiment: trajectory stored by the system attracted by the distractor and estimated trajectory to reach the position of the disappeared target. (a) Effect of the fading parameter  $F$  while recovering the target position. (b) The distractor was applied for different time windows from 0.5s to 2.5s

The trajectory stored by the architecture during the effect of the distractor and the estimated trajectory followed to reach the disappeared target are reported in Fig. 3.11 where the role of the fading parameter is underlined together with the effect of an increase in the distraction time.

### 3.4 Conclusions

In this chapter a computational model of the *Drosophila* ellipsoid body based on a four-ring spiking network is developed. The neural structure codes the heading direction using a hill of spiking activity in a ring-shaped structure. Simulation results show the capability of the system to store spatial position on a polar coordinate system. The proposed model is able to show behaviours similar to experiments with *Drosophila melanogaster* in the detour paradigm. Further details on the proposed architecture can be found in [2]; key elements contained in this model were subsequently found in the neural networks within the EB of *Drosophila* in biological experiments [16], further assessing the role of system models for a potential and fruitful subsequent biological assessment. Although the model was assessed only in simulation, the architecture proposed can be easily extended and applied on robotic roving/walking systems.

### References

1. Aradi, I., Barna, G., Erdi, P.: Chaos and learning in the olfactory bulb. *International Journal of Intelligent Systems* **10**(1), 89–117 (1995)
2. Arena, P., Maceo, S., Patané, L., Strauss, R.: A spiking network for spatial memory formation: Towards a fly-inspired ellipsoid body model. In: *The 2013 International Joint Conference on Neural Networks, IJCNN 2013, Dallas, TX, USA, August 4-9, 2013*, pp. 1–6 (2013). DOI 10.1109/IJCNN.2013.6706882. URL <http://dx.doi.org/10.1109/IJCNN.2013.6706882>
3. Arena, P., Mauro, G.D., Krause, T., Patané, L., Strauss, R.: A spiking network for body size learning inspired by the fruit fly. In: *The 2013 International Joint Conference on Neural Networks, IJCNN 2013, Dallas, TX, USA, August 4-9, 2013*, pp. 1–7 (2013). DOI 10.1109/IJCNN.2013.6706883. URL <http://dx.doi.org/10.1109/IJCNN.2013.6706883>
4. Arena, P., Patané, L., Strauss, R.: Motor learning and body size within an insect brain computational model. In: *Biomimetic and Biohybrid Systems - Third International Conference, Living Machines 2014, Milan, Italy, July 30 - August 1, 2014*. Proceedings, pp. 367–369 (2014)
5. Bisch-Knaden, S., Wehner, R.: Local vectors in desert ants: context-dependent landmark learning during outbound and homebound runs. *Journal of Comparative Physiology* **189**, 181–187 (2003)
6. Borenstein, J., Everett, H., Feng, L.: *Where am I? systems and methods for mobile robot positioning*. Technical Report (1996). URL <http://www-personal.umich.edu/~johannb/Papers/pos96rep.pdf>
7. Collett, M., Collett, T., Srinivasan, M.: Insect navigation: Measuring travel distance across ground and through air. *Current Biology* **16**, R887–R890 (2006)
8. Cruse, H., Wehner, R.: No need for a cognitive map: Decentralized memory for insect navigation. *PLoS Comput Biol* **7**(3), 1–10 (2011)

9. Haferlach, T., Wessnitzer, J., Mangan, M., Webb, B.: Evolving a neural model of insect path integration. *Adaptive Behavior* **15**, 273–287 (2007)
10. Hartmann, G., Wehner, R.: The ant's path integration system: a neural architecture. *Biological Cybernetics* **73**, 483–497 (1995)
11. Kahsai, L., Carlsson, M., Winther, A., Nassel, D.: Distribution of metabotropic receptors of serotonin, dopamine, GABA, glutamate, and short neuropeptide F in the central complex of *Drosophila*. *Neuroscience* **208**, 11–26 (2012)
12. Kuntz, S., Poeck, B., Strauss, R.: Visual working memory requires permissive and instructive NO/cGMP signaling at presynapses in the *Drosophila* central brain. *Current Biology* **27(5)**, 613–623 (2017)
13. Neuser, K., Triphan, T., Mronz, M., Poeck, B., Strauss, R.: Analysis of a spatial orientation memory in *Drosophila*. *Nature* **453**, 1244–1247 (2008)
14. Ofstad, T., Zuker, C., M.B., R.: Visual place learning in *Drosophila melanogaster*. *Nature* **474**, 204–209 (2011)
15. Redish, A., Elga, A., Touretzky, D.: A coupled attractor model of the rodent head direction system. *Network: computation in neural systems* **7(4)**, 671–685 (1996)
16. Seelig, J.D., Jayaraman, V.: Neural dynamics for landmark orientation and angular path integration. *Nature* **521(7551)**, 186–191 (2015). DOI doi:10.1038/nature14446
17. Song, P., Wang, X.: Angular path integration by moving hill of activity: A spiking neuron model without recurrent excitation of the head-direction system. *The Journal of Neuroscience* **25(4)**, 1002–1014 (2005)
18. Wehner, R.: Desert ant navigation: how miniature brains solve complex tasks. *Journal of Comparative Physiology A* **189**, 579–588 (2003)
19. Wittmann, T., Schwegler, H.: Path integration - a network model. *Biological Cybernetics* **73**, 569–575 (1995)
20. Wu, C., Xia, S., Fu, T., Wang, H., Chen, Y., Leong, D., Chiang, A., Tully, T.: Specific requirement of NMDA receptors for long-term memory consolidation in *Drosophila* ellipsoid body. *Nature Neuroscience* **10**, 1578–1586 (2007)
21. Young, J., Armstrong, J.: Structure of the adult central complex in *Drosophila*: Organization of distinct neuronal subsets. *The Journal of Comparative Neurology* **518**, 1500–1524 (2010)